

# Galactic 1.275 MeV emission from ONe novae and its detectability by INTEGRAL/SPI

P. Jean,<sup>1,2</sup> M. Hernanz,<sup>2</sup> J. Gómez-Gomar,<sup>2</sup> J. José,<sup>2,3</sup>

<sup>1</sup>Centre d'Etude Spatiale des Rayonnements, CNRS/UPS, 9 avenue du colonel Roche, 31028 Toulouse, FRANCE

<sup>2</sup>Institut d'Estudis Espacials de Catalunya (IEEC), CSIC, Gran Capità 2-4, E-08034 Barcelona, SPAIN

<sup>3</sup>Departament de Física i Enginyeria Nuclear (UPC), Av. Víctor Balaguer, s/n, E-08800 Vilanova i la Geltrú (Barcelona), SPAIN

Accepted 2000 March 29. Received 2000 March 7

## ABSTRACT

Models of Galactic 1.275 MeV emission produced by the decay of the radionuclide  $^{22}\text{Na}$  have been computed. Several frequency-spatial distributions of novae have been investigated using recent results of nova rates and spatial distributions of novae in our Galaxy. These models allow us to estimate the lower-limit of the  $^{22}\text{Na}$  mass ejected per ONe nova detectable with the future spectrometer (SPI) of the INTEGRAL observatory as a function of the frequency-spatial distribution of ONe novae in the Galaxy. Calculations using recent estimations of the expected  $^{22}\text{Na}$  mass ejected per ONe nova show that the detection of the Galactic emission of 1.275 MeV photons will be difficult with the future spectrometer of the INTEGRAL observatory, whereas the cumulative emission around the Galactic center has some chances to be detected during the deep survey of the central radian of the Galaxy.

**Key words:** gamma-rays: observations - novae, cataclysmic variables - white dwarfs - Galaxy: structure

## 1 INTRODUCTION

Observations with several instruments have provided upper-limits to the 1.275 MeV flux, related to  $^{22}\text{Na}$  decay from the Galaxy or from individual novae, (see Clayton & Hoyle (1974) for the original idea to look for  $^{22}\text{Na}$  lines in novae). Observations with the HEAO3  $\gamma$ -ray spectrometer provided an upper limit of  $4 \times 10^{-4}$  photons  $\text{cm}^{-2} \text{s}^{-1}$  on the Galactic accumulated flux at 1.275 MeV (Higdon & Fowler (1987), hereafter HF87). With the  $\gamma$ -ray spectrometer of the Solar Maximum Mission, Leising et al. (1988) found a 99% confidence limit of  $1.2 \times 10^{-4}$  photons  $\text{cm}^{-2} \text{s}^{-1}$  on a steady 1.275 MeV flux from the Galactic center direction. Iyudin et al. (1995), using observations of single novae, with the COMPTEL instrument on board the Compton Gamma-Ray Observatory, estimated a  $2\sigma$  upper-limit of  $3 \times 10^{-5}$  photons  $\text{cm}^{-2} \text{s}^{-1}$  for any neon-type nova in the Galactic disk, which has been translated into an upper-limit of the ejected  $^{22}\text{Na}$  mass of  $3.7 \cdot 10^{-8} M_{\odot}$ .

The next generation of  $\gamma$ -ray spectrometers will have the sensitivity required for the detection of the 1.275 MeV emission from classical ONe novae. In particular, SPI, the future spectrometer of the INTEGRAL observatory will be operational in 2001. With its high energy resolution ( $\Delta E/E \approx 0.2\%$ ), the spectrometer is designed for the detection of astrophysical  $\gamma$ -ray lines in the 20 keV - 8 MeV energy range.

The detection plane is made of 19 germanium (Ge) detectors and is surrounded by an active shield made with bismuth germanate (BGO) scintillators, in order to reduce the instrumental background. SPI will be able to perform images with an angular resolution of  $\approx 3^{\circ}$  by using a coded aperture system made of tungsten elements. The mean fully coded field-of-view is  $\approx 16^{\circ}$  (for a more detailed description of the spectrometer see Mandrou et al. (1997) and Teegarden et al. (1997)). Using calculations of  $^{22}\text{Na}$  yields in ONe novae by José & Hernanz (1998) and instrumental background predictions, Hernanz et al. (1997) and Gómez-Gomar et al. (1998) estimated that the 1.275 MeV line from an individual ONe nova could be detected by SPI if its distance is less than  $\approx 0.5$  kpc (*standard* CO novae produce  $^{22}\text{Na}$  in much smaller amounts than ONe novae). With a new analysis of the nuclear reaction rates involved in  $^{22}\text{Na}$  synthesis (José, Coc & Hernanz 1999) a bit larger distance is obtained (around 1.5 kpc, Hernanz et al. (1999)).

The total Galactic flux at 1.275 MeV depends not only on the amount of  $^{22}\text{Na}$  ejected per outburst but also on the distribution and the rate of Galactic ONe novae. However, the Galactic nova rate is poorly known, independently of the underlying white dwarf composition, because the interstellar extinction prevents us from directly observing more than a small fraction of the novae that explode each year. Several methods have been used to estimate the nova occur-

rence rate. Estimations based on extrapolations of Galactic nova observations suggest a rate in the range 50-100 yr<sup>-1</sup> (see Liller & Mayer (1987) and references therein). Observations of novae in other galaxies have revealed a correlation between the nova rate and the infrared luminosity of the parent galaxy. However, the occurrence rates of Galactic novae computed by scaling the nova rate measured in external galaxies are lower than  $\approx 50$  yr<sup>-1</sup>. With this method, Ciardullo et al. (1990) predicted a nova rate in the range 11-45 yr<sup>-1</sup>, and Della Valle & Livio (1994) a rate  $\approx 20$  yr<sup>-1</sup>. This is significantly lower than estimations based on Galactic nova observations. Recently, Shafter (1997) reconciled this difference by recomputing the nova rate with the Galactic nova data. He extrapolated the global nova rate from the observed one, accounting for surface brightnesses of the bulge and the disk components and correction factors taking care of any observational incompleteness. With this method, Shafter (1997) estimated the nova rate to be  $35 \pm 11$  yr<sup>-1</sup>. Hatano et al. (1997) found a similar value ( $41 \pm 20$  yr<sup>-1</sup>) using a Monte-Carlo technique with a simple model for the distribution of dust and classical novae in the Galaxy. As only ONe novae are important producers of <sup>22</sup>Na, the Galactic ONe nova rate is the relevant one for this work. The Galactic ONe nova rate is obtained by multiplying the total nova rate by the fraction of novae that results from thermonuclear runaways on ONe white dwarfs. Williams et al. (1985) deduced from observations of abundances in nova ejecta a proportion of ONe novae from 20 to 40 percent. With a detailed model of white dwarf mass distribution in cataclysmic binaries, Ritter et al. (1991) estimated that 25-57 percent of observed nova outbursts should occur on ONe white dwarfs. Livio & Truran (1994) reestimated the frequency of occurrence of ONe novae, in light of observations of abundances in nova ejecta. They concluded that, of the 18 classical novae for which detailed abundance analyses were available, only two or three had a large amount of neon and were ONe novae, whereas three other novae showed a modest enrichment in neon, casting doubt on the type of the underlying white dwarf. Under these considerations, they estimated a fraction of Galactic ONe novae between 11 and 33 percent.

In addition to the <sup>22</sup>Na mass ejected per outburst and the ONe novae rate, the distribution of ONe novae in the Galaxy is an important parameter that tunes the total 1.275 MeV flux arriving on Earth. Some <sup>22</sup>Na mass upper-limits, resulting from 1.275 MeV total Galactic flux upper-limit measurements, are underestimated since they have been computed assuming that all the ONe novae are embedded in the Galactic Center. Indeed, a larger <sup>22</sup>Na mass can be ejected by ONe novae leading to a 1.275 MeV total Galactic flux below the measured upper-limit if the ONe nova distribution is more diluted in the Galaxy.

In this paper, we model the Galactic cumulative emission at 1.275 MeV as a function of the ONe novae rate and the mean <sup>22</sup>Na yield per outburst, for several spatial distributions of novae in the Galaxy. The lower-limit for the mean mass yield of <sup>22</sup>Na ejected per nova, in order to detect the 1.275 MeV cumulative emission, is predicted for the future observations of SPI, using the estimation of the sensitivity of the future spectrometer developed by Jean (1996) and Jean et al. (1997). The method for the simulation of the Galactic 1.275 MeV emission and its results are described in section 2, whereas the method of observation with SPI and

its application to the previous simulations are presented in section 3. Discussion and conclusions follow (section 4).

## 2 SIMULATION OF THE GALACTIC 1.275 MeV EMISSION

### 2.1 Method

The 1.275 MeV emission from Galactic ONe novae is calculated with a Monte-Carlo simulation. A simulation of a set of ONe novae that is representative of what could be the Galactic novae distribution at a given time, i.e. a given novae frequency-spatial distribution, is made (this set of novae is further called a ‘Galaxy-test’). The two nova populations (bulge and disk) have been considered. The population origin (bulge or disk), the position in galacto-centric coordinates (depending on the chosen population) and the age of ONe novae are chosen randomly according to the appropriate distributions. The local-galactic coordinates ( $l, b$ ) of each nova as well as its distance to the Sun are calculated assuming a Sun to Galactic center (hereafter GC) distance of 8 kpc. The 1.275 MeV flux ( $F_{22}$  in photons cm<sup>-2</sup> s<sup>-1</sup>) has been estimated using the relationship

$$F_{22} = 3.17 \cdot 10^5 \frac{M_{22} e^{-\frac{t}{\tau_{22}}}}{A_{22} \tau_{22} d^2} \quad (1)$$

where  $M_{22}$  is the <sup>22</sup>Na mass ejected per nova (in solar masses),  $t$  the age of the nova (in years),  $d$  its distance to the Sun (in kpc).  $A_{22}$  and  $\tau_{22}$  are the mass number and the lifetime of <sup>22</sup>Na (3.75 yr), respectively. Limitation of the flux due to opacity of the ejecta has not been taken into account, since it is significant only in the first week after the explosion (Gómez-Gomar et al. 1998), which is a short time as compared to the <sup>22</sup>Na lifetime. The number of simulated ONe novae depends on the global (CO and ONe) nova frequency ( $f_n$ ), the total period during which ejected <sup>22</sup>Na is an effective emitter ( $N_\tau \tau_{22}$ ), the proportion of novae in the bulge ( $p_b$ ) and the proportion of ONe novae in the bulge (with respect to all novae in the bulge,  $q_b$ ) and in the disk (with respect to all novae in the disk,  $q_d$ ). The number of simulated ONe novae is calculated as

$$N_n = f_n N_\tau \tau_{22} [p_b q_b + (1 - p_b) q_d] \quad (2)$$

It has been assumed that the emissivity of novae older than  $5\tau_{22}$  has a negligible contribution to the diffuse Galactic 1.275 MeV emission; therefore,  $N_\tau=5$ . The proportion of ONe novae in the bulge (with respect to all ONe novae) is given by

$$p_{ONe}^{bulge} = \frac{p_b q_b}{p_b q_b + (1 - p_b) q_d} \quad (3)$$

The simulation of a Galaxy-test provides a set of 1.275 MeV line fluxes  $F_i$  for each nova  $i$  localized at  $l_i, b_i$ . Distribution of the intensity and of the number of novae has been calculated with 3° by 3° size pixels, which correspond to the angular resolution of SPI.

### 2.2 Models

### 2.2.1 Distribution of novae in the Galaxy

For the purpose of this work, a Galaxy model with a disk and a spheroid is convenient to simulate the distribution of Galactic nova events. Several laws for the spatial distribution in the disk and in the ‘spheroid’ (representative of the bulge) have been proposed in the literature. We have selected four models that differ significantly from each other. The first and older of them is described in Higdon & Fowler (1987). The radial scalelength of the disk is derived from the starlight surface brightness distribution (de Vaucouleurs & Pence 1978) and the height dependence is from Patterson (1984). HF87 use the analytic dependence for the spheroid light distribution from Bahcall et al. (1982) and Young (1976), also called the ‘ $R^{1/4}$ ’ law ( $R$  is the distance to the GC), originally formulated by de Vaucouleurs (1948). By scaling the nova rate in the bulge of M31 to the bulge of our Galaxy, HF87 estimate a proportion of novae in the spheroid of 0.348. The second model has been used by Hatano et al. (1997) to estimate the spatial distribution and the occurrence rate of Galactic classical novae. It is based on a model of the distribution of type Ia supernovae (Dawson & Johnson 1994). The proportion of novae that occur in the bulge is set to 0.111 on the basis of an estimate of the bulge to total galaxy mass ratio. The third model is derived from the Galactic survey of the Spacelab InfraRed Telescope (IRT) that provides a reliable tracer of the distribution of G and K giant stars (see Kent, Dame & Fazio (1991) and Kent (1992)). It has also been used by Prantzos & Diehl (1996) to estimate the contribution of old population stars (novae and AGB) to the Galactic  $^{26}\text{Al}$  emission at 1.8 MeV measured by COMPTEL. Using the total infrared luminosity of the bulge and the disk, the derived proportion of novae occurring in the bulge is 0.179. The last model is taken from Van der Kruit (1990). It has been used by Shafter (1997) to estimate the nova rate in our Galaxy. This author assumes that the nova distribution follows the brightness profile of our Galaxy. Under this assumption, the proportion of bulge novae is 0.105.

The adopted distributions are shown in Figures 1, 2 and 3, which represent the probability to find a nova in the Galactic bulge at spherical radius  $R$  in a volume element ( $\text{kpc}^{-3}$ , Figure 1), and the probabilities to find a nova in the Galactic disk at cylindrical radius  $\rho$  in an area element ( $\text{kpc}^{-2}$ , Figure 2) and at height  $z$  above the Galactic plane in a line element ( $\text{kpc}^{-1}$ , Figure 3). Table 1 summarizes the characteristics of the adopted models.

### 2.2.2 Galactic ONe nova rate

As presented in section 1, methods used to estimate the occurrence rate of novae are based on extragalactic and Galactic nova observations. The first method can underestimate the Galactic nova rate since the nova count can be biased by the extinction of the Galactic disk. On the other hand, estimations obtained with Galactic nova observations depend on the Galaxy model used for the extrapolation. The last estimations of classical novae rates are those by Shafter (1997) ( $35 \pm 11 \text{ yr}^{-1}$ ) and Hatano et al. (1997) ( $40 \pm 20 \text{ yr}^{-1}$ ). Therefore, for the calculations presented in section 2.3, we have adopted frequencies of Galactic novae ranging from  $20 \text{ yr}^{-1}$  to  $60 \text{ yr}^{-1}$  and a proportion of ONe novae from 10 % to

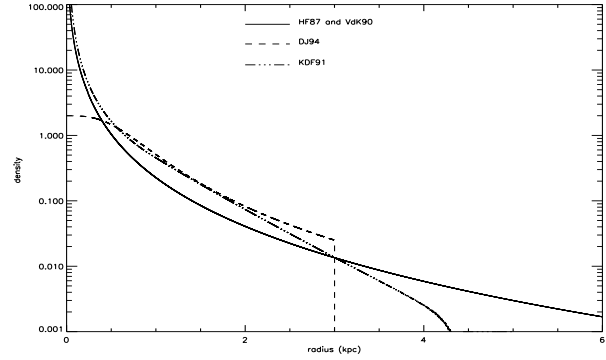


**Figure 1.** Radial distributions of novae in the Galactic bulge for four models (in  $\text{kpc}^{-3}$ ). HF87: model used by Higdon & Fowler (1987) derived from the spheroid light distribution. This last model has also been adopted by Van der Kruit, 1990 (VdK90). KDF91: model from Kent, Dame and Fazio (1994) corresponding to the distribution of G and K giant stars provided by the InfraRed Telescope observations. DJ94: model from Dawson and Johnson (1994) derived from the distribution of type Ia supernovae. This last model has been truncated at 3 kpc (see table 1 for details).

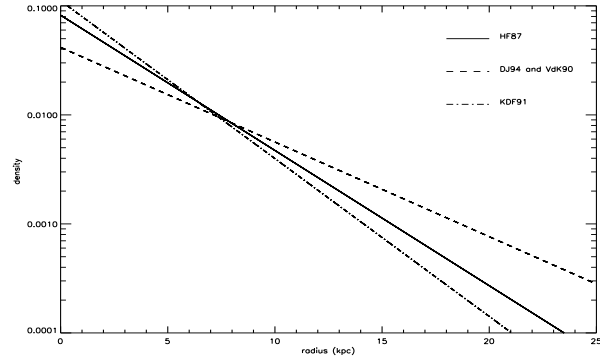


**Figure 2.** Radial distributions (cylindrical coordinate) of novae in the Galactic disk (in  $\text{kpc}^{-2}$ ) for the four models discussed in figure 1 (see text for details).

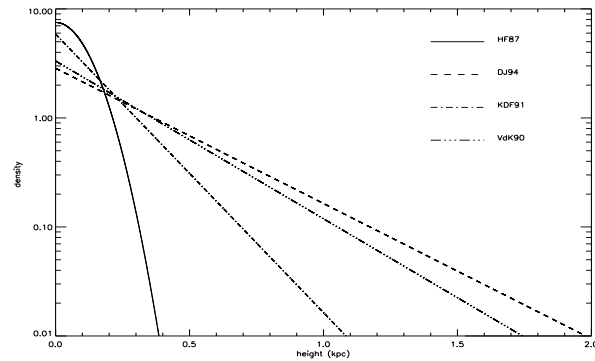


**Figure 3.** Height above the Galactic plane distributions (cylindrical coordinate) of novae in the Galactic disk (in  $\text{kpc}^{-1}$ ) for the four models discussed in figure 1 (see text for details).

**Table 1.** Nova spatial distributions used for the simulation of the Galactic 1.275 MeV emission.  $R$  is the distance to the GC,  $z$  is the distance perpendicular to the Galactic plane and  $\rho$  is the galactocentric planar distance. The distance from the GC to the Sun is  $R_\odot=8$  kpc,  $n_s$  and  $n_d$  are the normalization factors for the spheroid and the disk respectively (in  $\text{kpc}^{-3}$ ). The proportions of novae in the spheroid,  $p_b$ , are 0.348 (HF87), 0.105 (VdK90), 0.179 (KDF91) and 0.111 (DJ94)

Model HF87:  $\rho_h=3.5$  kpc and  $z_o=0.106$  kpc.

$$\begin{aligned} \text{Disk } n(z, \rho) &= n_d e^{-\frac{1}{2} \frac{z^2}{z_o^2} - \frac{\rho}{\rho_h}} \\ \text{Bulge } n(R) &= n_s 1.25 \left( \frac{R}{R_\odot} \right)^{-\frac{6}{8}} e^{-10.093 \left( \frac{R}{R_\odot} \right)^{\frac{1}{4}} + 10.093} & R \leq R_\odot \\ &= n_s \left( \frac{R}{R_\odot} \right)^{-\frac{7}{8}} \left[ 1 - \frac{0.0867}{\left( \frac{R}{R_\odot} \right)^{\frac{1}{4}}} \right] e^{-10.093 \left( \frac{R}{R_\odot} \right)^{\frac{1}{4}} + 10.093} & R \geq R_\odot \end{aligned}$$

Model VdK90:  $\rho_h=5.0$  kpc and  $z_h=0.30$  kpc.

$$\begin{aligned} \text{Disk } n(z, \rho) &= n_d e^{-\frac{|z|}{z_h} - \frac{\rho}{\rho_h}} \\ \text{Bulge } n(R) &= n_s 1.25 \left( \frac{R}{R_\odot} \right)^{-\frac{6}{8}} e^{-10.093 \left( \frac{R}{R_\odot} \right)^{\frac{1}{4}} + 10.093} & R \leq R_\odot \\ &= n_s \left( \frac{R}{R_\odot} \right)^{-\frac{7}{8}} \left[ 1 - \frac{0.0867}{\left( \frac{R}{R_\odot} \right)^{\frac{1}{4}}} \right] e^{-10.093 \left( \frac{R}{R_\odot} \right)^{\frac{1}{4}} + 10.093} & R \geq R_\odot \end{aligned}$$

Model KDF91:  $\rho_h=3.0$  kpc and  $z_h=0.170$  kpc.  $K_0$  is the modified Bessel function.

$$\begin{aligned} \text{Disk } n(z, \rho) &= n_d e^{-\frac{|z|}{z_h} - \frac{\rho}{\rho_h}} \\ \text{Bulge } n(R) &= n_s 1.04 \times 10^6 \left( \frac{R}{0.482} \right)^{-1.85} & R \leq 0.938 \text{ kpc} \\ &= n_s 3.53 K_0 \left( \frac{R}{0.667} \right) & R \geq 0.938 \text{ kpc} \\ &= 0 & R \geq 5 \text{ kpc} \end{aligned}$$

Model DJ94:  $\rho_h=5.0$  kpc and  $z_h=0.35$  kpc.

$$\begin{aligned} \text{Disk } n(z, \rho) &= n_d e^{-\frac{|z|}{z_h} - \frac{\rho}{\rho_h}} \\ \text{Bulge } n(R) &= \frac{n_s}{R^{3+0.343}} & R \leq 3 \text{ kpc} \\ &= 0 & R \geq 3 \text{ kpc} \end{aligned}$$

30 %, in agreement with the recent estimate (Livio & Truran 1994). These values correspond to a lower and upper limit of the ONe nova rate of  $2 \text{ yr}^{-1}$  and  $18 \text{ yr}^{-1}$ , respectively.

### 2.2.3 $^{22}\text{Na}$ yield range

The most recent upper-limit for the  $^{22}\text{Na}$  mass ejected by ONe novae is provided by Iyudin et al. (1995), who derived  $3 \cdot 10^{-8} M_\odot$  for any neon-type nova in the Galactic disk, at a  $2\sigma$  level with COMPTEL. Recent theoretical estimations (José & Hernanz 1998) provide typical  $^{22}\text{Na}$  yields of  $\approx 2 \cdot 10^{-9} M_\odot$  per ONe nova, well below such observational upper limit. However, the average yield of  $^{22}\text{Na}$  ejected per nova is not yet well known. It is sensitive to the composition of the underlying white dwarf and to the degree of mixing between the core and the accreted envelope (which constrain not only the ejected envelope mass but also the maximum temperature reached during the runaway) and also to the convection efficiency (Starrfield et al. 1998), (José & Hernanz 1998). It is important to remind that in some cases theoretical models predict total ejected masses which are smaller than some observed ones (which in turn have often large determination uncertainties). Moreover, some uncertainties of nuclear reaction cross-sections affect the computed  $^{22}\text{Na}$  yields: a net increase in the  $^{22}\text{Na}$  ejected mass by a typical ONe nova is obtained, with a very recent update of the nuclear reaction network affecting  $^{22}\text{Na}$  synthesis. The new  $^{22}\text{Na}$  yields for typical ONe novae are larger by factors ranging between  $\sim 2$  and  $\sim 10$ , resulting in ejected masses as

large as  $10^{-8} M_\odot$  for a  $1.25 M_\odot$  ONe nova in the most favorable case of nuclear reaction rates (José, Coc & Hernanz 1999).

### 2.3 Results: maps of the 1.275 MeV emission

Examples of Galaxy-tests for the distributions of novae in the Galaxy presented in section 2.2.1 are shown in Figures 4, 5, 6 and 7. For these simulations, the adopted Galactic nova rate is  $35 \text{ yr}^{-1}$  (Shafter 1997) and the proportion of ONe novae is 30%. As already shown by HF87, the 1.275 MeV intensity is irregularly distributed in the Galaxy. We have recovered the  $^{22}\text{Na}$  upper-limit mass found by HF87 with the sensitivity of HEAO3 -  $4 \cdot 10^{-4} \text{ photons cm}^{-2} \text{ s}^{-1}$  at a  $3\sigma$  level, (Mahoney et al. 1982) - by simulating their frequency-spatial distribution of Galactic novae (rate  $46 \text{ yr}^{-1}$  and spatial distribution as shown in Table 1) and by integrating the flux between  $330^\circ$  and  $30^\circ$  longitude.

The statistical distributions of the 1.275 MeV fluxes from the  $12.5^\circ$  around the GC and from the brightest nova of the Galaxy have been calculated using a large number of Galaxy-tests. The results are presented in figure 8 and 9 for an ONe nova rate of  $\approx 10 \text{ yr}^{-1}$  and for the four models of spatial distribution. The KDF91 model provides the highest mean flux in the GC region, whereas the distribution of fluxes emitted by the brightest nova are similar in the four models, since the distributions of novae distances to the Sun are similar up to  $\approx 7$  kpc for all the models.

Table 2 shows the mean 1.275 MeV flux from the GC entering in the SPI field-of-view normalized to the  $^{22}\text{Na}$  mass

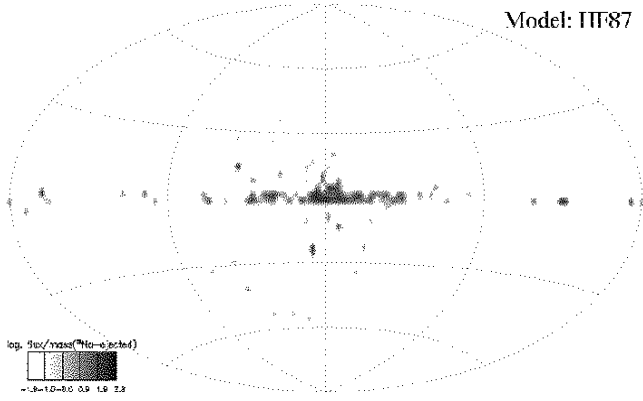


**Figure 4.** Example of modeled diffuse 1.275 MeV emission generated by a Monte Carlo simulation for the HF87 model. The fluxes have been normalized with the  $^{22}\text{Na}$  ejected mass (photons  $\text{s}^{-1} \text{cm}^{-2} M_{\odot}^{-1}$ ). The relative intensity is plotted with  $3^{\circ}$  by  $3^{\circ}$  pixels in a map in galactic coordinates. For this example of Galaxy-test, the adopted ONe nova rate is  $\approx 10 \text{ yr}^{-1}$ .

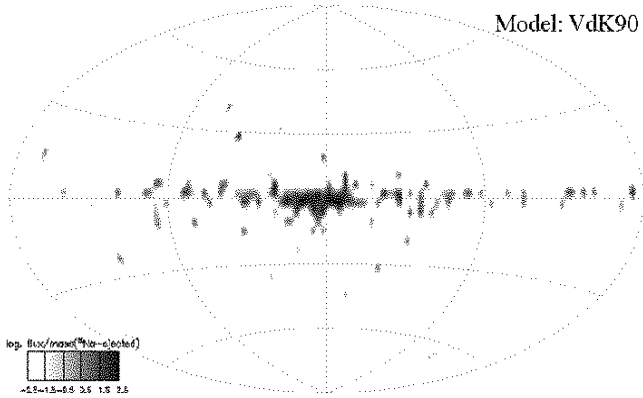


**Figure 5.** Same as figure 4 but for the VdK90 model.

ejected per year in the Galaxy. The uncertainties give an idea of the intensity fluctuation magnitude due to the limited number of effective emitting novae in the SPI field-of-view. The normalized fluxes are directly related to the spatial characteristics of the chosen Galactic ONe novae distribution (see Table 1). The total 1.275 MeV normalized flux of the Galaxy is also presented in Table 2. The intensity in

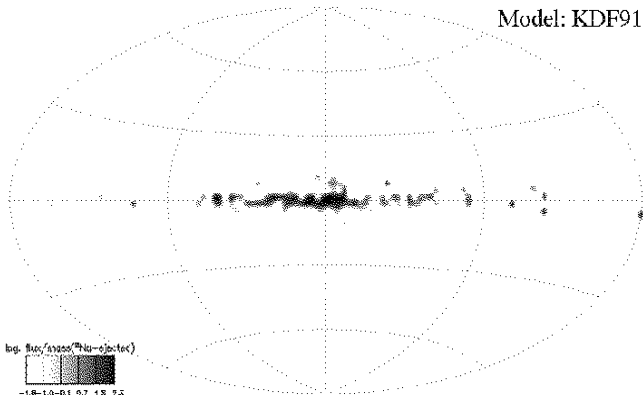


**Figure 6.** Same as figure 4 but for the KDF91 model.

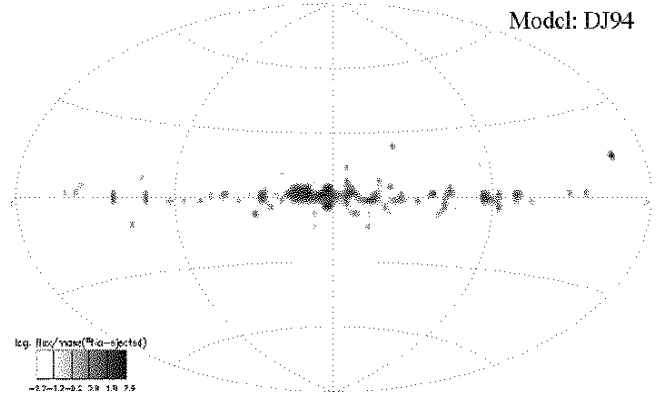


**Figure 7.** Same as figure 4 but for the DJ94 model.

**Table 2.** Mean simulated 1.275 MeV flux emitted by ONe novae in the  $12.5^{\circ}$  around the GC region and in the whole Galaxy. The flux  $F_N$  is normalized to the  $^{22}\text{Na}$  mass ejected per outburst and the rate of Galactic ONe novae (photons  $\text{cm}^{-2} \text{s}^{-1} M_{\odot}^{-1} \text{yr}$ ). Values correspond to the four adopted models.

Models	$F_N(GC)$	$F_N(Total)$
HF87	$78.0 \pm 2.4$	$507 \pm 85$
VdK90	$56.8 \pm 3.5$	$580 \pm 287$
KDF91	$105.1 \pm 2.9$	$508 \pm 62$
DJ94	$56.4 \pm 1.4$	$496 \pm 119$

the GC region represents 15%, 10%, 21% and 11% of the total flux in the Galaxy for the HF87, VdK90, KDF91 and DJ94 models, respectively.

We have investigated the variation of the normalized 1.275 MeV intensity in the  $12.5^{\circ}$  around the GC as a function of the scaleheight and scalelength of the novae distributions in the case of a zero proportion of novae in the bulge (see below). For a 0.3 kpc scaleheight, the normalized intensity decreases from  $\approx 89$  to  $\approx 31$  photons  $\text{cm}^{-2} \text{s}^{-1} M_{\odot}^{-1} \text{yr}$  when the scalelength increases from 2.5 to 6.0 kpc. Although the novae distances to the Sun are decreasing with increasing scalelength, the distribution around the GC is more diluted and the flux entering in the field-of-view is therefore lower.

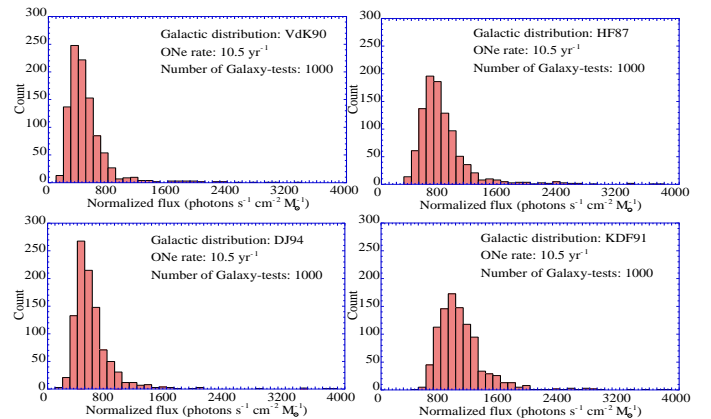


**Figure 8.** Histogram of the normalized flux (flux per  $^{22}\text{Na}$  ejected mass per outburst) in the  $12.5^{\circ}$  around the GC obtained from 1000 simulated Galaxy-tests. The four models of spatial distribution are presented.

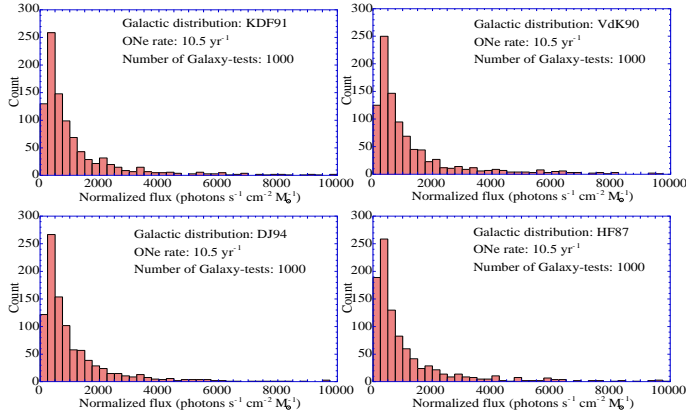


**Figure 9.** Histogram of the normalized flux (flux per  $^{22}\text{Na}$  ejected mass per outburst) emitted by the brightest ONe novae of the Galaxy. The four models of spatial distribution are presented.

### 3 ANALYSIS OF THE GALACTIC 1.275 MeV EMISSION BY SPI

#### 3.1 Types of detection

Each one of the above mentioned Galaxy-tests could be observed by a  $\gamma$ -ray spectrometer at a given date. This is true if the observation time is short as compared with the occurrence period of ONe novae and with the time variation of the  $^{22}\text{Na}$  emissivity. These conditions are satisfied since the common observation time of the future  $\gamma$ -ray spectrometer SPI will be  $\approx 11$  days, that is shorter than both the average ONe novae occurrence period ( $\approx 45$  days) in the whole Galaxy, and the decay period of  $^{22}\text{Na}$  (3.75 yr, implying 1.275 MeV flux reduction of only 0.8% in 11 days). However, for an observation time longer than few times the ONe novae occurrence period, the time variation of the 1.275 MeV Galactic emissivity has to be accounted for. Figure 10 shows an example of the total 1.275 MeV flux variations in the  $12.5^\circ$  around the GC. It results from a Monte Carlo simulation as described in the previous section. The flux has been normalized to the  $^{22}\text{Na}$  ejected mass per outburst. In figure 10, the flux in the GC is dominated by a single nova (which contributes to 91% of the total flux) at 8.6 yr. After 20 yr, the flux shows fluctuations with a maximum amplitude of  $\pm 40\%$  of the mean flux. Figure 11 shows the statistical distributions of the relative variations between two epochs of the total 1.275 MeV flux in the  $12.5^\circ$  around the GC. They have been calculated using the flux variation of figure 10. Several delays between the two epochs are presented. For two observations 6 months apart, there are probabilities of 15% and 21% to get a flux variation of more than 10% and less than -10% respectively. Even if the flux variations are not large, the weak additional spots that could appear in the field-of-view will modify the distribution of the pixel-intensity. This could modify significantly the analysis in the case of the detection of excesses in the spatial distribution (see section 3.1.2).

As stated above (section 2.1), the number of novae and the distribution of the intensity have been calculated with  $3^\circ$  by  $3^\circ$  pixels. Therefore, several novae can be located in the same pixel (this happens mostly in the direction of the GC region). However, the flux in those pixels can be dominated

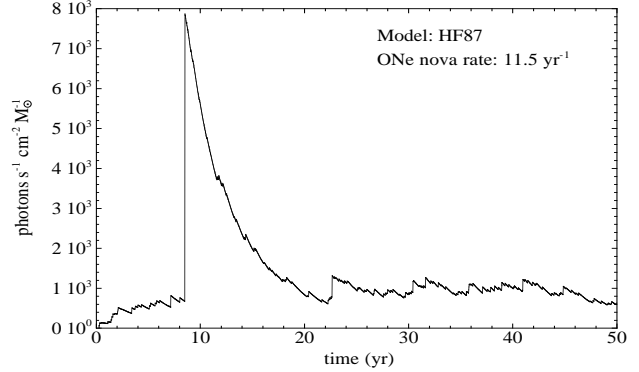


**Figure 10.** Example of the total 1.275 MeV normalized flux in the  $12.5^\circ$  around the GC as a function of time. This results from a simulation with the HF87 model and an ONe nova rate of  $11.5 \text{ yr}^{-1}$ . The flux in the GC can be dominated by a single close nova.

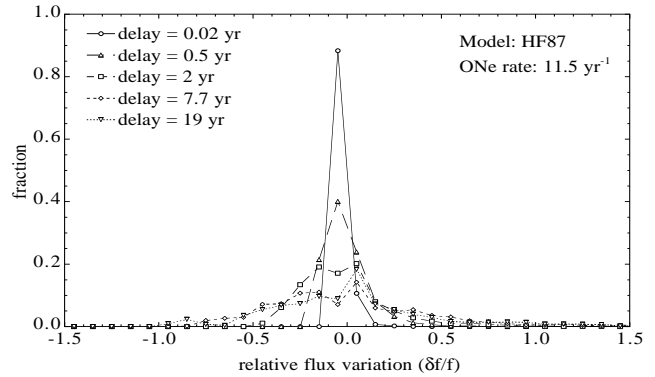


**Figure 11.** Distributions of the relative variations of the 1.275 MeV normalized flux in the  $12.5^\circ$  around the GC between two observations separated by delays of 0.02 yr, 0.5 yr, 2 yr, 7.7 yr and 19 yr. These distributions are obtained with the light curve presented in figure 10.

by only one nova. In this case, the measured intensity can not be considered as a cumulative effect. Therefore, we state for a seldom-nova criterium when a single nova contributes to more than 95% of the total flux in a pixel.

Jean (1996) and Jean et al. (1997) have estimated the narrow line sensitivity of SPI for an on-axis point source by computing instrumental background and detection efficiency with Monte-Carlo simulations including detailed physics. However, Gómez-Gomar et al. (1998) have shown that the 1.275 MeV line should have a typical width of 20 keV (FWHM). With these conditions, the sensitivity is  $2.2 \cdot 10^{-5}$  photons  $\text{cm}^{-2} \text{ s}^{-1}$  at a  $3\sigma$  level and for  $10^6$  s ( $\approx 11$  days) of observation time, instead of  $6 \cdot 10^{-6}$  photons  $\text{cm}^{-2} \text{ s}^{-1}$ . In the present case, the Galactic ONe novae emission is diffuse and the spectrometer will also provide a distribution of intensity in pixels.

Therefore, three types of detection have been investigated for the analysis of any Galaxy-test.

### 3.1.1 Detection of the cumulative emission at 1.275 MeV (case 1)

The total 1.275 MeV flux impinging on the SPI detectors will generate counts that will be added to the instrumental background ones. It will be possible to estimate these source counts by subtracting the instrumental background component from the overall detector rates without using imaging deconvolution. Contrary to the imaging method, where the background rate is estimated using detectors that are not illuminated by a source (i.e. half of the total number of detectors - which are below opaque mask elements), the instrumental background is estimated using either observations pointing out of the galactic plane - i.e. the on/off method used in balloon-borne spectrometers - or background modelling. The latter can consist of estimating the instrumental background under the line of interest either by using data obtained during the observation (rate around the studied line, other background feature rates), or by fitting the background temporal variations before and after the observations, or both of the two methods.

For this study, we simply consider the measurement of the cumulative emission with the on/off method. The sensitivity is estimated using the calculation of Jean (1996) (see also SPI - Science Performance Report (SPI - Science Performance Report 1996)) assuming that the time spent to measure instrumental background is equal to the GC observation time and that there is no more modulation of the source photons by the coded aperture. In this case the exposure is on average equal to the point source exposure since half of the flux irradiates the detection plane (the other half being hidden by the coded mask elements). Since the counts recorded over all the detectors are taken into account, the background is increased by a factor  $\approx 2$  with respect to the imaging case. Therefore, since the sensitivity increases with the square root of the background, the sensitivity of such a mode of detection is roughly the sensitivity for an on-axis point source (in the imaging case) multiplied by the square-root of 2 (i.e.  $3.1 \cdot 10^{-5}$  photons  $\text{cm}^{-2} \text{s}^{-1}$  at a  $3\sigma$  level and for  $10^6$  s of observation time). In this method, the single information that will be available is the number of detected 1.275 MeV photons coming from the region in the field-of-view of SPI. Although such a detection will give the proof of  $^{22}\text{Na}$  decay in the Galaxy, it will not provide any information on its spatial distribution in the observed region. However, galactic  $^{22}\text{Na}$  yield can be estimated provided that assumptions on the ONe distribution in the Galaxy are made.

### 3.1.2 Detection of excesses in the spatial distribution of the intensity at 1.275 MeV (case 2)

The total flux in the SPI field-of-view is distributed in several pixels. Some of the pixels can contain an intensity that leads to a significant signal. In this case, we obtain an additional information that is the location of the emission in the Galaxy. However, it is necessary to account for the reduction of the significance of the detection with the number of pixels involved in the total flux. A rough estimation of the significance (number of  $\sigma$ ) of such a detection is derived by computing the probability that the observed intensity distribution in the field-of-view is due to background fluctuation. The lower the probability, the higher the significance.

The number of sigma for each pixel is calculated by comparing the flux with the sensitivity for a point source (Jean et al. 1997). Afterwards, this number of sigma is converted in probabilities. The combination of the probabilities of the overall pixels allows us to estimate the probability that the observed distribution is not due to background fluctuation. Equation 4 shows an estimation of this probability  $P$  that is available when the significances in pixels are high enough.  $N$  is the total number of pixels in the SPI field-of-view,  $k$  is the number of pixels above a given significance threshold ( $2.5\sigma$  in this work) and  $P_i$  is the probability derived from the significance in the pixel  $i$ .

$$P = \frac{N!}{(N-k)!} \prod_{i=1}^k P_i \quad (4)$$

The distribution of the emission from the GC is considered to be detected when the calculated probability leads to a significance that is above  $3\sigma$  for an observation time of  $10^6$  seconds ( $\approx 11$  days). A single nova close to the Earth can be the major source in the SPI GC field-of-view. Account for such an event makes a bias on the statistics of the cumulative 1.275 MeV flux. Therefore, to avoid such effect, the effective single nova pixel is removed from the analysis if its flux is more than 95% of the central  $25^\circ$  total flux.

### 3.1.3 Detection of the brightest nova of the Galaxy in 1.275 MeV (case 3)

The flux from the brightest nova that can be observed from the Earth is also analyzed and considered to be detected if its value is above the sensitivity of the spectrometer SPI, for an observation time of  $\approx 11$  days. The observation time needed to detect with SPI (at a  $3\sigma$  level) the brightest nova of the Galaxy-test has also been estimated. Equation (5) allows us to calculate the duration of the observation ( $T_{3\sigma}$  in days) to get a  $3\sigma$  detection of the flux  $f$  (photons  $\text{cm}^{-2} \text{s}^{-1}$ ) in a single pixel.

$$T_{3\sigma} = 2.42 \cdot 10^{-5} f^{-1} + 5.28 \cdot 10^{-9} f^{-2} \quad (5)$$

We can recognize the well known variation of the sensitivity as a function of the square root of the observation time in the second term of the equation, that is dominant when the signal-to-noise ratio is low (i.e. low fluxes). The first term accounts for the statistical fluctuations induced by the counts from sources when the signal-to-noise ratio is not low anymore (i.e. for high fluxes).

## 3.2 Probability to detect the 1.275 MeV line with SPI

For a large number of Galaxy-tests, the probability to detect any type of emission can be estimated by calculating the fraction of time that the simulated 1.275 MeV flux is above the upper-limit of a given experiment (HEAO3 or SPI). For the particular case of the future spectrometer of INTEGRAL, the average times of observation to obtain detections of the three types mentioned above have been derived, as well as the average number of novae that contribute to the diffuse emission of the GC region. Each Galaxy-test has been analyzed in order to check whether SPI would detect: the cumulative emission at 1.275 MeV in the  $12.5^\circ$

around the GC region (case 1), an excess in the distribution of the emission (case 2) and the brightest nova of the Galaxy (case 3), for a given average  $^{22}\text{Na}$  yield per ONe nova outburst. The time needed for a  $3\sigma$  level detection is also computed. Two hundred Galaxy-tests have been simulated for each model and for a given  $^{22}\text{Na}$  yield in order to calculate the number of Galaxy-tests that lead to a detection by SPI with an observation time of  $10^6$  s. The number obtained, divided by the total number of Galaxy-tests, gives an estimation of the probability to detect the 1.275 MeV line from ONe novae with SPI.

Figure 12 shows the mean observation times for the three types of detection with SPI, as a function of the average  $^{22}\text{Na}$  mass ejected per nova. The adopted ONe nova rate is  $10 \text{ yr}^{-1}$  and the spatial distributions of novae are those described in section 2.2.1. For low values of  $^{22}\text{Na}$  yield, the observation times are very long and do not make sense since the limited duration of the INTEGRAL mission does not allow for observation times larger than 2 years. Moreover, as the Galactic 1.275 MeV intensity and its distribution would change due to the decay of  $^{22}\text{Na}$  and to the explosion of additional novae, the analysis of the intensity distribution (case 2) and of the brightest nova flux (case 3) are not valid anymore. However, other analyses (cases 1) can be possible with exposures in the limit of the allocated observation time.

Figure 13 shows the fraction of time that SPI would detect, in  $\approx 11$  days, an excess in the distribution of the emission from the GC region (case 2) as a function of average  $^{22}\text{Na}$  masses ejected per nova, for Galactic ONe nova rates ranging from 2 to  $18 \text{ yr}^{-1}$  (i.e., an estimation of the probability to detect this emission). In this analysis, it is not possible to normalize the  $^{22}\text{Na}$  mass ejected by the ONe nova rate, because when the frequency of novae increases, the  $(l, b)$  distribution of intensity changes, resulting in an estimation of the significance that implies more pixels and not only more flux. Therefore, the sensitivity to an excess in the 1.275 MeV intensity distribution is not directly proportional to the amount of  $^{22}\text{Na}$  ejected per year.

Our results allow for the determination of the  $^{22}\text{Na}$  yield lower-limit that can be detected by the spectrometer of INTEGRAL. We state that this lower-limit of  $^{22}\text{Na}$  ejected mass corresponds to a probability of detection of 90%. The lower-limit depends also on the nova rate, since more ONe novae lead to higher cumulative GC region flux, on the Galaxy model and on the type of detection. Taking the  $^{22}\text{Na}$  mass values at 90% of probability in Figure 13 we can calculate the lower-limit as a function of the Galactic ONe nova rate for case 2. Similar calculations have been performed for the detection of the cumulative emission in the SPI field-of-view (case 1) and of the brightest nova of the Galaxy (case 3). The results are displayed in Figures 14 for the four adopted spatial distributions, as a function of the nova rate. As it has already been shown in Figure 12, it is clear that the future spectrometer SPI will be more sensitive to the brightest nova of the Galaxy and the total diffuse flux than to a detection of an excess in the distribution of the emission. The  $^{22}\text{Na}$  lower-limit masses needed to detect the brightest nova (case 3) are similar for the four models, since the distributions of novae distances to the Sun associated to these models are similar up to  $\approx 7$  kpc from the Sun. Concerning the  $^{22}\text{Na}$  lower-limit masses for the cumulative emission (case 1), it can be seen in Figure

14 that models KDF91 and HF87 provide lower values than VdK90 and DJ94 models. The radial scalelengths for the former are 3.0 kpc and 3.5 kpc, respectively, whereas the models VdK90 and DJ94 have higher radial scalelengths, 5 kpc in both cases (see Table 1). Since novae are closer to the GC in the KDF91 and HF87 models, their cumulative 1.275 MeV flux is higher and more compact (see Figures 4, 5, 6 and 7). For a given ONe nova rate, the  $^{22}\text{Na}$  lower-limit mass decreases with decreasing scaleheight of the Galactic disk: the lower the  $z_h$  (i.e., models HF87 and KDF91), the higher the cumulative 1.275 MeV flux at the GC (see Table 2) and the smaller the  $^{22}\text{Na}$  lower-limit mass (see Figure 14). However, this variation is not significant: for instance, when the scaleheight increases from 0.1 kpc to 0.45 kpc the  $^{22}\text{Na}$  lower-limit mass increases from  $\approx 7 \cdot 10^{-7} M_{\odot}$  to  $9 \cdot 10^{-7} M_{\odot}$ , if we use the DJ94 model with variable scaleheight. Moreover, the limited angular resolution of SPI constrains to a lower-limit the observable disk scaleheight. Indeed, in the case of an exponential disk model (without bulge contribution), simulations show that the estimated  $^{22}\text{Na}$  lower-limit mass does not change for  $z_h$  values lower than  $\approx 0.15$  kpc and  $\approx 0.25$  kpc, which correspond roughly to a scale-angle of  $3^{\circ}$  for a Galactic disk radial scalelength of 5 kpc and 3 kpc, respectively.

It is not clear whether the Galactic bulge should be a source of 1.275 MeV photons, since it has been proposed that it is  $10^{10}$  years old and white dwarfs responsible of ONe novae should be much younger (the zero age mass of the white dwarf progenitor being probably larger than  $\sim 10 M_{\odot}$ ). However, the ages of novae do not only depend on the main sequence lifetime of the progenitor but also on the time necessary for the onset of the Roche lobe overflow in the binary system and the time between the onset of accretion and the outburst phase. Taking into account the eventuality that there is a lack of ONe novae in the bulge (see the recent paper by Della & Livio (1998)), we have estimated the  $^{22}\text{Na}$  mass lower-limits in the case of ONe novae only distributed in the Galactic disk. Figure 15 shows the results of the simulations in this case for the four models adopted: the  $^{22}\text{Na}$  mass lower-limits that SPI can detect are in general lower, since novae are concentrated in the disk and, therefore, they are closer to the Earth.

As a final result, extracted from those presented in Figure 12, Figure 16 shows the observation time needed to have 90% of chance to detect with SPI the 1.275 MeV line emitted by the accumulated  $^{22}\text{Na}$  from the GC region (case 1) as a function of the mean  $^{22}\text{Na}$  mass ejected per ONe nova. These results are displayed for the four distributions of novae in the Galaxy. For the HF87 and KDF91 spatial distributions and our estimations of  $^{22}\text{Na}$  yields, observation times compatible with those planned for the deep survey of the central Galaxy are obtained. Therefore, cumulative emission in the GC may be detected with SPI.

## 4 DISCUSSION AND CONCLUSIONS

It is important to remind that the total Galactic flux at 1.275 MeV depends not only on the amount of  $^{22}\text{Na}$  ejected per outburst and the ONe nova rate but also on their distribution in the Galaxy. The ejected  $^{22}\text{Na}$  mass upper-limit derived by HF87 using HEAO3 measurement was estimated for

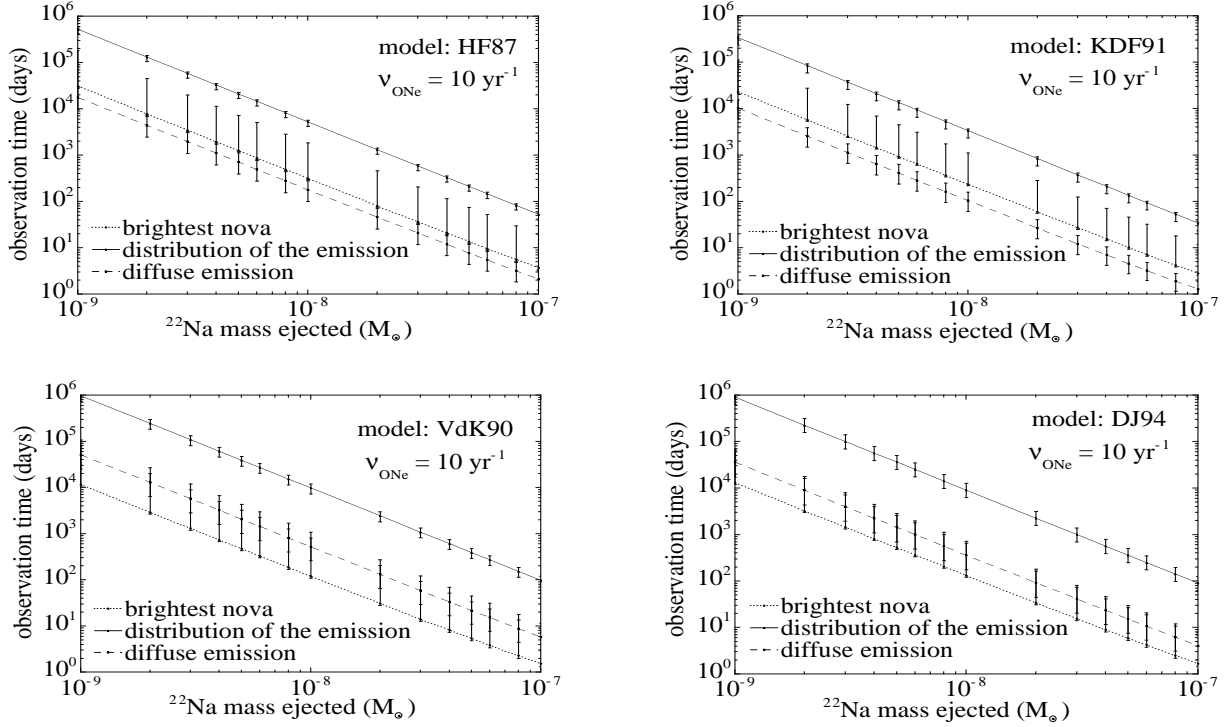


**Figure 12.** Mean observation time needed to detect the cumulative (diffuse) emission in the GC (case 1), the distribution of the emission (case 2) and the brightest nova (case 3) at 1.275 MeV with the future spectrometer SPI, as a function of the mean  $^{22}\text{Na}$  yield per nova. The error bars have a width of  $1\sigma$ . The adopted Galactic ONe nova rate is  $10 \text{ yr}^{-1}$ . Each point results from the processing of 200 Galaxy-tests. Each panel corresponds to a different spatial distribution of novae (see text for details).

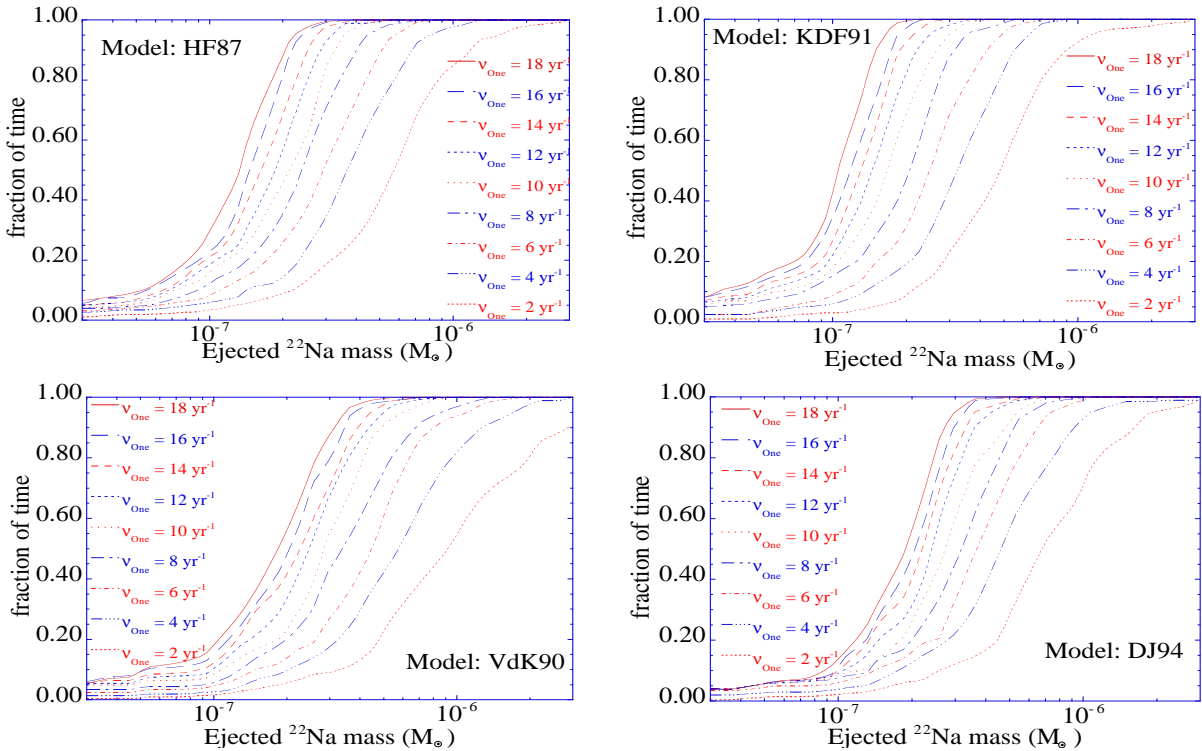


**Figure 13.** Fraction of time during which the distribution of the diffuse emission, in a sphere of  $25^\circ$  diameter around the GC would be detected by SPI (case 2), as a function of mean  $^{22}\text{Na}$  yields per nova, calculated for ONe nova rates ranging from 2 to  $18 \text{ yr}^{-1}$  and for the four adopted Galaxy models. Each point results from the processing of 200 Galaxy-tests.

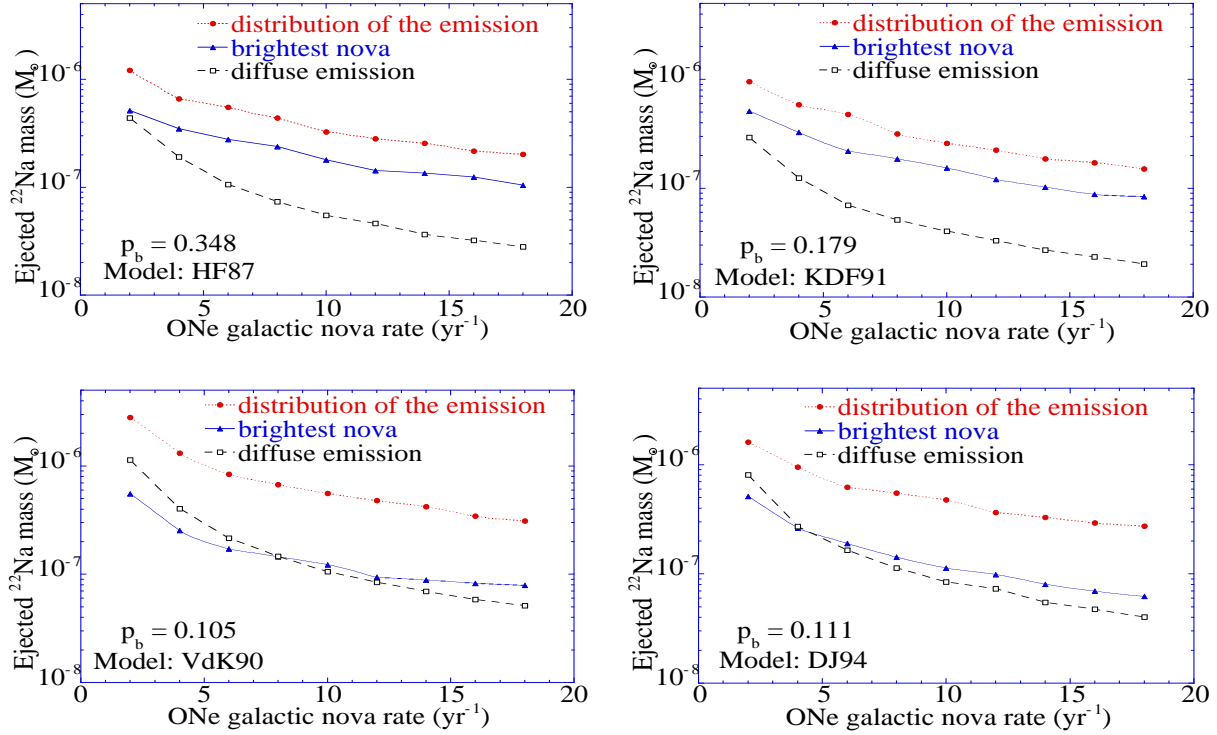


**Figure 14.** Lower-limits of the  $^{22}\text{Na}$  mass ejected per nova that can lead to 90% of probability that the 1.275 MeV emission, from the novae in the GC region (total flux -case 1- and distribution -case 2) and from the brightest nova of the Galaxy (case 3), will be detected with SPI at a  $3\sigma$  level in  $10^6$  s of observation, as a function of the ONe nova rate.

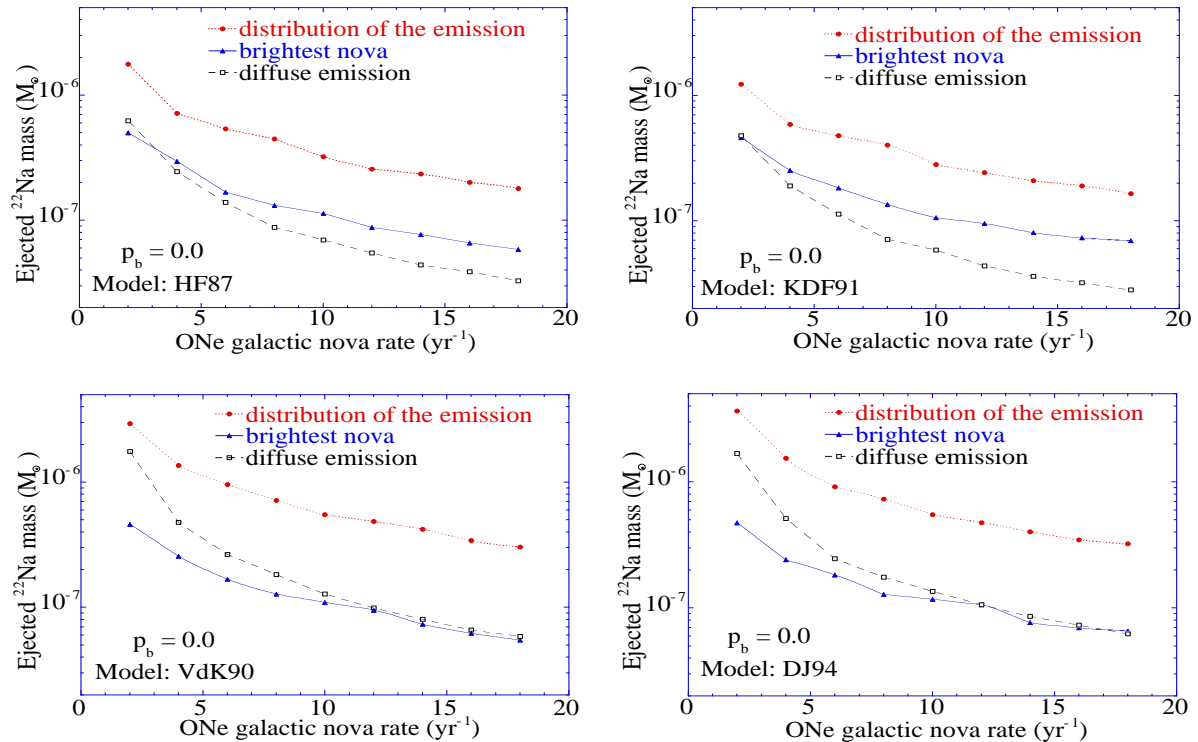


**Figure 15.** Same as figure 14 but without ONe novae occurring in the bulge.

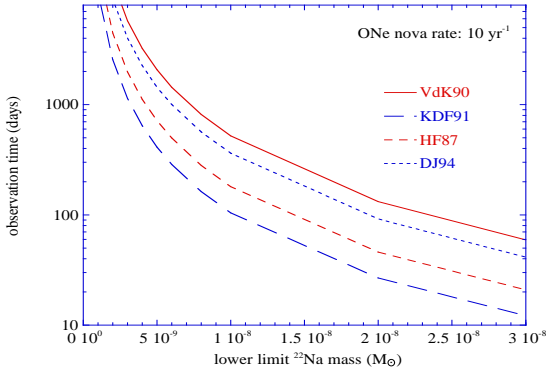


**Figure 16.** SPI observation time necessary to have 90% of chance to detect the cumulative 1.275 MeV emission of the GC (case 1) as a function of the mean  $^{22}\text{Na}$  mass ejected per nova and for several Galactic distributions.

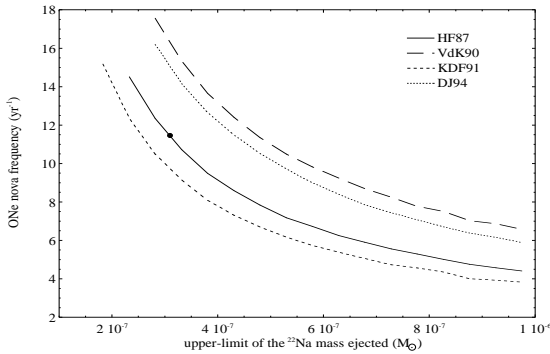


**Figure 17.** Galactic ONe nova rate needed to have 90% of chance to detect the cumulative 1.275 MeV emission from the GC region (between  $330^\circ$  and  $30^\circ$ ) with HEAO3 as a function of the mean  $^{22}\text{Na}$  mass ejected per nova and for several Galactic distributions. The dot shows the estimation of HF87.

only one distribution and an ONe nova rate of  $11.5 \text{ yr}^{-1}$ . Figure 17 shows the  $^{22}\text{Na}$  mass upper-limits computed with the 1.275 MeV upper-limit flux of HEAO3 considering other possible frequency-spatial distributions of novae in the Galaxy. It shows that the  $^{22}\text{Na}$  mass upper-limit lies between  $2$  and  $10 \cdot 10^{-7} M_\odot$  per nova.

The spectrometer of INTEGRAL will be more sensitive for the detection of the brightest nova of the Galaxy and of the cumulative diffuse emission of ONe novae in the GC region by an “on-off” type observation than for the determination of their intensity distribution. But it is not clear whether the brightest novae will be first detected in the visible due to the interstellar extinction. Nevertheless, long exposures in the Galactic plane region may allow for their detection with SPI.

According to José, Coc & Hernanz (1999), the  $^{22}\text{Na}$  average yield could be between  $3 \cdot 10^{-9}$  and  $1.2 \cdot 10^{-8} M_\odot$  per nova. Therefore, there are few chances to detect the Galactic diffuse 1.275 MeV emission with SPI with only  $\approx 10$  days of observation. However, 80 days of observation of the GC region could already give constraints to the mean  $^{22}\text{Na}$  yield in ONe novae as a function of their frequency-spatial distribution in the Galaxy (see Figure 16).

It is worth mentioning that the adopted width of the

1.275 MeV line (20 keV) is quite large, corresponding to the fastest ONe novae, which have the largest ejection velocities (and also the largest ejected  $^{22}\text{Na}$  masses). As the correlation between  $^{22}\text{Na}$  ejected mass and ejection velocity is not well established (neither theoretically nor observationally), and the braking of the ejected mass during the lifetime of  $^{22}\text{Na}$  is in principle small but not null, we are in the worst situation when we adopt such broad lines (corresponding to the largest velocities and without any braking effect). In the other extreme case of narrow lines (less realistic but interesting to make a comparison), the sensitivity of SPI is  $6 \cdot 10^{-6}$  photons  $\text{cm}^{-2} \text{ s}^{-1}$  at a  $3\sigma$  level and for  $10^6 \text{ s}$  ( $\approx 11$  days) of observation time, for a point source, which is  $\sim 3.7$  times better than the one for our broad lines (see section 3.1) and allows for the detection of lower fluxes by the same factor. Consequently, a positive detection of the 1.275 MeV line by SPI would be achieved either with a smaller  $^{22}\text{Na}$  mass or with a smaller observation time.

Gamma-ray observation of novae would provide information not only on their eruption mechanisms and the nucleosynthesis processes involved in their explosion but also on their distribution and their rate in the Galaxy (e.g. proportion in the bulge, scaleheight in the Galactic disk) since the problem of the interstellar extinction does not appear at this energy range.

## ACKNOWLEDGMENTS

We wish to thank G. Skinner for his helpful comments.

Research partially supported by the training and Mobility Researchers Programme, ‘Access to supercomputing facilities for european researchers’, established between the European Community and CESA-CEPBA, under contract ERBFMGECT050062, and with the research projects ESP98-1348 (CICYT-PNIE), PB97-0983-C03-02 and PB97-0983-C03-03 (DGICYT), GRQ94-8001 (CIRIT).

## REFERENCES

- Bahcall J. N., Schmidt M., Soneira R. M. 1982, ApJ, 258, L23–L27
- Ciardullo R. et al., 1990, AJ, 99, 1079
- Clayton D. D., Hoyle F., 1974, ApJ, 187, L101–L103
- Dawson P. C., Johnson R. G., 1994, JRASC, 88, 369
- de Vaucouleurs G., 1948, Ann. d’Astrophys., 11, 247
- de Vaucouleurs G., Pence W., 1978, AJ, 83, 1163
- Della Valle M., Livio M., 1994, AAP, 286, 786–788
- Della Valle M., Livio M., 1998, ApJ, 506, 818–823
- Della Valle M., Bianchini A., Livio M., Orio M. 1992, AAP, 266, 232–236
- Gómez-Gomar J., Hernanz M., José J., Isern J., 1998, MNRAS, 296, 913–920
- Hatano K., Branch D., Fisher A., 1997, ApJ, 487, L45–L48
- Hatano K., Branch D., Fisher A. & Starrfield S. 1997, MNRAS, 290, 113–118
- Hernanz M., Gómez-Gomar J., José J., Isern J., 1997, Proceedings of the 2<sup>nd</sup> INTEGRAL Workshop, ESA publication division, 382, 47
- Hernanz M., Gómez-Gomar J., José J., Coc A., Isern J., 1999, Astrophysical Lett. & Communications, 38, 407
- Higdon J. C., Fowler W. A., 1987, ApJ, 317, 710–716
- Iyudin A. F., et al., 1995, AAP, 300, 422

- Jean P., 1996, PhD Thesis
- Jean P., Naya J., von Ballmoos P., Vedrenne G., Teegarden B., 1997, Proceedings of the 2<sup>nd</sup> INTEGRAL Workshop, ESA publication division, 382, 635
- José J., Hernanz M., 1998, ApJ, 494, 680–690
- José J., Coc A., Hernanz M., 1999, ApJ, 520, 347
- Kent S. M., 1992, ApJ, 387, 181–188
- Kent S. M., Dame T. M., Fazio G., 1991, ApJ, 378, 131–138
- Leising M. D., Share G. H., Chupp E. L., Kanbach G., 1988, ApJ, 328, 755–762
- Liller W., Mayer B., 1987, PASP, 99, 606
- Livio M., Truran J. W., 1994, ApJ, 425, 797–801
- Mahoney W. A., Ling J. C., Jacobson A. S., Lingenfelter R. E., 1982, ApJ, 262, 742
- Mandrou P. et al., 1997, Proceedings of the 2<sup>nd</sup> INTEGRAL Workshop, ESA publication division, 382, 591
- Patterson J., 1984, ApJs, 54, 443–493
- Prantzos N., Diehl R., 1996, Phys. Rep., 267, 1–69
- Ritter H., Politano M., Livio M., Webbink R. F., 1991, ApJ, 376, 177–185
- Shafter A. W., 1997, ApJ, 487, 226
- SPI - Science Performance Report, 1996, SPI-NS-0-9758-CSCI
- Starrfield S., Truran J.W., Wiescher M.C., Sparks W.M., 1998, MNRAS, 296, 502
- Teegarden B. et al., 1997, AIP Proceedings of the fourth Compton Symposium, eds. C.D. Dermer, M.S. Strickman and J.D. Kurfess, 410, 1535
- Van der Kruit P., 1990, in The Milky Way as a Galaxy, ed. R. Buser & I.R. King (Mill Valley: University Science Books), page 331
- Williams R. E., Ney E. P., Sparks W. M., Starrfield S. G., Wyckoff S., Truran J. W., 1985, MNRAS, 212, 753–766
- Young P., 1976, AJ, 81, 807